

Received January 27, 2021, accepted February 8, 2021, date of publication February 18, 2021, date of current version March 2, 2021.

Digital Object Identifier 10.1109/ACCESS.2021.3060315

# Robust Data Predictive Control Framework for Smart Multi-Microgrid Energy Dispatch Considering Electricity Market Uncertainty

IBRAHIM BRAHMIA<sup>1</sup>, JINGCHENG WANG<sup>1,2</sup>, HAOTIAN XU<sup>1</sup>,  
HONGYUAN WANG<sup>1</sup>, AND LUCA DE OLIVEIRA TURCI<sup>1</sup>

<sup>1</sup>Department of Automation, Shanghai Jiao Tong University, Shanghai 200240, China

<sup>2</sup>Autonomous Systems and Intelligent Control International Joint Research Center, Xi'an Technological University, Xi'an 710021, China

Corresponding author: Jingcheng Wang (jcwang@sjtu.edu.cn)

This work was supported in part by the National Natural Science Foundation of China under Grant 61533013 and Grant 61633019, and in part by the Shaanxi Provincial Key Project under Grant 2018ZDXMGY-168.

**ABSTRACT** With the emerging technologies for Energy Intent (EI) and data-driven applications, the conventional power grid network is undergoing a radical modernization. An efficient energy management and electricity price forecasting remains a challenging task. In this paper, a new Robust Data Predictive Control framework for Energy Management System (RDPC-EMS) is developed to overcome the uncertainty of the electricity retail price market and minimize the total operating costs for the multi-microgrids (MMG) system. The proposed framework solves the economic energy dispatch based on an accurate Electricity Price Forecasting (EPF) by an Outlier-Robust Extreme Learning Machine (OR-ELM) algorithm and a two layers cooperative Distributed Model Predictive Control (DMPC). The First level provides an optimal energy scheduling between the Distribution System Operator (DSO) and cooperative microgrids systems to minimize the operating cost based on the forecasted electricity price. In contrast, second level maintains the supply-demand balance by applying the optimal energy scheduling from the first layer through an adjustment of the distributed energy resources (DER). The electricity retail price prediction is assessed using real dataset from the Iso New England electricity market. The OR-ELM regression method shows a significant forecasting performance in terms of error metrics. For instance, the mean absolute error in the training stage 2.05% for OR-ELM with a comparison of 4.17% and 6.29% for Support Vector Regression (SVR), and Artificial Neural Network (ANN) models respectively. Finally, simulation results demonstrate the efficiency RDPC-EMS for daily operating cost reduction, with decrease of 15% for MG 1 and 16% for MG 2.

**INDEX TERMS** Distributed model predictive control, energy management, outlier robust extreme learning machine, renewable energy sources, retail electricity price market.

## NOMENCLATURE

### ACRONYMS

MPC	Model Predictive Control
DMPC	Distributed Model predictive Control
EMS	Energy Management System
SVR	Support Vector Regression
ELM	Extreme Learning Machine
OR-ELM	Outlier Robust Extreme learning Machine

SLFN	Single Layer Feed Forward Neural Network
ANN	Artificial Neural Network
MMG	Multi- Microgrid System
MG	Microgrid
DER	Distributed Energy Resources
PV	Photovoltaic System
WT	Wind Turbine
DG	Diesel Generator unit
LMP	Locational Marginal Price
EPF	Electricity Price Forecasting
DSO	Distribution System Operator

The associate editor coordinating the review of this manuscript and approving it for publication was Arup Kumar Goswami.

**NOTATION**

$p_{grid}$	Power from the grid
$p^b$	Power from the battery
$\overline{p}_i^b$	Maximum power from battery
$\underline{p}_i^b$	Minimum power from battery
$p_i^{SL}$	Flexible load
$p_i^{CL}$	Critical load
$p_i^L$	Total active load
$p_i^{DG}$	Power generated for diesel generators
$p_i^{RES}$	Power generated form renewable resources
$p_i^S$	Energy mismatch
$p_i^{surp}$	Energy surplus
$k$	Time interval index
$E_i^{chr}$	Charging energy of battery
$E_i^{dch}$	Discharge energy of battery
$\eta_i$	Conversion efficiency of battery
$C$	Constant parameter of the regularization
$\Delta t$	Duration of each period in hours
$\delta_{i,k}$	Binary variable tem[e] The training error
$R^2$	Coefficient of determination
MAE	Mean absolute error [cents/KWh]
MAPE	Mean absolute percentage error [%]
RMSE	Root means square error [cents/KWh]

**I. INTRODUCTION**

Toward smart and sustainable cities, an adoption of clean power generation is rising steeply worldwide. The availability of Distributed energy resource (DER) including renewable energy provide a promising solutions, to address the climate and energy crisis, and the new technological advances have caused an outstanding reduction in electricity prices. As a result, smart grids systems are meant to replace conventional power network, and offer an Eco-friendly environment with intelligent distribution system [1]. One of the specific paradigms in optimal energy resources control is the so-called Multi-Microgrids (MMG) systems [2], which cover the defect of single Microgrid (MG), and expand the potential usage based on cooperative energy management and dispatch. The most important advantage of MMG is the ability to utilize the DER, and the energy surplus among MMG network instead of producing all the required energy independently [3]. In addition, as a result of the cooperative mechanism minimize the total operating costs for MMG. Furthermore, the system operators can invest in other aspect of the operation because of cost reduction. For instance, enhance security and reliability of the power network [4].

Demand-side energy production is one of the key for efficient energy management among MMGs power plants, however, it is based on the operation mode [5], which it can occur as standalone MGs or grid-connected mode. Regarding the new edge of energy trading technology and the increase of cooperative residential MGs, nowadays in academia and industry, the Distribution System Operator (DSO) is considered the key for efficient and smooth energy management. For instance, in [6] authors proposed bi-level energy

scheduling for multiple home energy hubs as well as energy purchase/sale mechanism. Authors in [7] propose another approach with two layers of energy management have been introduced, where a bi-level decentralized distribution management systems (DMS). Moreover, a stochastic multi-objective approach for energy management of MMGs is suggested in [8]. However, demand-side management has not been taken into account. To fill the gap of authors in [9] develop an advanced retail electricity market for day-ahead energy exchanged based on a scenario of virtual power plants competes with electricity retailers with bids/offers principle.

The model-based paradigm for microgrids energy management and architecture has been heavily studied [10]. A recent article [11] suggest a smart optimization based on fuzzy control for residential microgrids system, as in literature [12] authors studied the dispatch energy among the MMGs systems employing particle swarm optimization (PSO) algorithm, however this type of optimization known with their computation complexity and low convergence solutions. The article [13] proposed an evolutionary adaptive dynamic programming integrating frequency control for networked MG system. Renewable energy is considered an essential part of the microgrid's supply power, such as solar radiation and wind speed, which often fluctuate because of weather uncertainty. As a result, the energy storage devices are essential to maintain the MGs operations [14]. The objective of energy management approaches in cooperative MMG consists of obtaining an optimal distribution of controllable load generators with efficient Power-sharing in case of demand-supply mismatch. However, the main weakness of the mentioned approaches is the high computational time when considering stochasticity and a large amount of data.

Additionally, as one of the popular model-based methods, Model predictive control (MPC) has also been proposed as a suitable and efficient solution for energy management and economic dispatch problems [15]. For example, in [16] robust MPC is proposed for energy management while satisfying time-varying request and operation constraints using Mixed-Integer Linear Programming (MILP) for modeling the overall optimization, another MPC approach presented in [17] as a two-layers MPC strategy for charging electric vehicles EVs connected to the microgrid. In [18] a robust hierarchical MPC with three control levels including frequency control for autonomous smart MGs. Authors in [19], [20] propose an interesting research articles, for the optimal energy scheduling of multi-microgrid system connected to the main grid based on two stage stochastic MPC which compromise a centralize entity to compute operating energy dispatch as first layer, and an efficient power management operation at each local microgrid system, taking into account different sources of uncertainties. Likewise, in [21] a novel method based on Chance Constrained MPC involving Gaussian Probability Distribution Function (PDF) under uncertainties parameters to provide a robust MMG-EMS. Further, an MPC design based on two-Layer optimization presented in [22] with a

two-stages algorithm with economic analysis for islanded microgrids considering the storage batteries degradation costs. In [23], a stochastic problem is combined in a model predictive control structure to compensate for the uncertainty with a feedback mechanism. To overcome the weakness of a centralized framework and the massive amount of control inputs/decision for microgrids networks. The distributed MPC has been employed for energy management and smart grids applications. In [24] a DMPC approach is employed to compute the amount of active power that should be exchanged among interconnected MMG. In addition, in [25] propose a resilient optimal solution for the power dispatch and reduce the economic costs. Also, for a multi-microgrids system, in the research presented by Du *et al.* [26] using DMPC based aggregators to handle the surplus energy trading between microgrids operating in autonomous mode. Despite the successful application of MPC, the electricity market uncertainty may cause high operating costs by not effectively schedule the microgrids systems.

In recent years, data-driven based machine learning approaches have been proposed for smart grids. For instance, in [27], the electricity price greatly affects decision making and energy dispatch and planning. Therefore, several forecasting methods have been developed. For instance, authors in [28] propose a comparative study Support Vector Regression (SVR) for short-term electricity prices forecasting based on support vector regression and Auto-regressive. Another approach in [29] suggest an annual forecast of power load based on a hybrid model based on SVR and nature-inspired algorithm Moth-Flame Optimization (MFO). Artificial neural network (ANN) is considered a classic regression model. For example, in [30] authors employed a hybrid ANN algorithm electricity market to effectively regulate the bidding strategies based on demand-side management (DSM). In [31] an Accurate Electricity price Forecasting (EPF) strategy based on long-short term memory (LSTM) for forecasting the electricity markets of Pennsylvania-New Jersey-Maryland. In [32] authors develop an advanced retail electricity market among the multiple competing players for reconfigurable networked MG system. However, the presence of the outliers in the electricity data has been introduced in [33] which investigates the substantial impact of the extreme outliers observations for the electricity market based on real data from the European Energy Exchange (EEX). The outlier robust extreme learning machine has been employed in a recent article for the electricity price forecast in [34], which exhibit an outstanding performance in data processing and regression modeling. The previous approach OR-ELM is based on the well-known Extreme Learning Machine (ELM) that has been used in several literature and studies. For example, authors in [35] forecast the PV power for real solar-power plant, and results show an outstanding result compared to the Artificial Neural Network (ANN) and SVR. Furthermore, in [36], dynamic pricing of a household has been forecasted based on ELM and ANN. In [37] combination strategy of MPC and

data-driven framework is proposed using random forest for building energy.

Although the extensive research that has been carried out for the MMG-EMS problems, and to the best of our knowledge, no research has been investigated the combination of the OR-ELM with DMPC optimization to solve MMG-EMS optimization considering electricity retail market uncertainty. Therefore, in this paper we propose a hybrid leaning optimization for smart energy distribution of cooperative residential microgrids community operation. We extend our previous work in [38] based on DMPC for autonomous multi microgrids energy management. Also, in [39] two layers energy management without considering electricity volatility. In this paper, a hybrid approach based on data-driven regression models and MPC has been employed for accurate EPF, with efficient energy management. Moreover, we adopt a cooperative tow layer with DSO as the first layer, and local controller as second layer to optimize global costs globally and locally for each MG with interaction among DSO-MG. The proposed hybrid optimization illustrate significant potential for the economic performance, and efficient energy scheduling for different MMG-EMS in grid-connected mode. The main contributions of this paper are as follows:

- Smart economic energy dispatch framework RDPC-EMS based on OR-ELM and DMPC considering electricity price market volatility. Further, maximize the use of RES with the advantage of the surplus power-sharing policy among the MMG system, and maintain the supply-demand while reduce the daily operating costs.
- An Accurate EPF based on the novel OR-ELM regression model with fast computation time and Lowest errors metric compared to conventional machine learning approaches SVR and ANN.
- Resilient energy distribution for the short-term day ahead energy scheduling can operate in cooperative and non-cooperative optimization, using real PV energy generation data from the Green Laboratory Building, and retail electricity price from the New England market.
- In our work, the EPF is based on historical data from the wholesale market, without undercover the user identity or information. Also, the DMPC algorithm is often implemented on edge devices such as Programmable language Controllers (PLC) which have the ability of setting up an end to end point encryption. Therefore, our strategy can be seen as solution to enhance privacy and cybersecurity for smart grids networks.

This paper is arranged as follows. In section II, system description. In section III Dynamic modeling and component are presented. In section IV, a description for the OR-ELM regression model for the electricity price forecasting following by an evaluation performance with ANN and SVR. In section V, the The two-level RDPC-EMS algorithm is formulated, with prove of stability and convergence. In section VI, a simulation is carried out. The conclusion and future work are given in section VII.

## II. SYSTEM DESCRIPTION AND DATA-SET

### A. SYSTEM OVERVIEW

Fig. 1 illustrates a typical cooperative smart MMG community interacting between each other by exchange power and information. Each MG compromise of a renewable energy source such as Wind Turbines (WT), and photovoltaic (PV) solar panels, plus energy storage systems and diesel generators, the DERs units are connected to a demand load from a smart building. In each MG architecture, local controller consider as the principal part responsible for energy scheduling. Each LC receive an optimal energy scheduling from DSO. Simultaneously, MMG exchanged information between and execute the reference planning for day-ahead energy management. The main objective of DSO is to predict the retail electricity price, and minimize the daily operating costs of the whole plant. Furthermore, the energy trading between DSO and the main grid is based on maximizing profit for each MG.

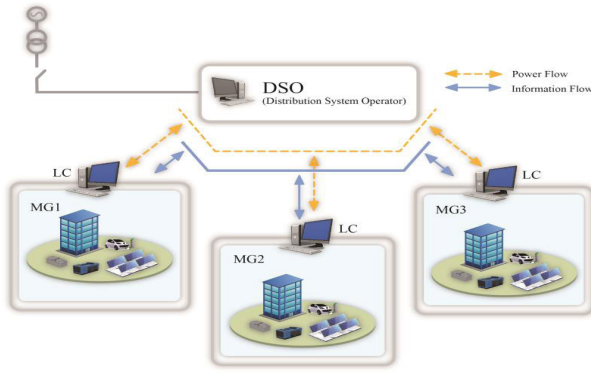


FIGURE 1. Cooperative residential smart microgrids community.

### B. SITE DESCRIPTION AND DATA SET

Historical data were collected from Monocrystalline PV Solar Panels on the rooftop of Green Energy Laboratory (GEL) Shanghai Jiao Tong university. China [40]. The geographical location is  $31^{\circ} 9' 27.5''$  N,  $121^{\circ} 21' 4.9''$  E. Further, for the retail electricity price, we employed the LMP hourly historical data (cents/KWh) from ISO New England [41] electricity market.

## III. DYNAMIC MODELING AND COMPONENTS

### A. INTERACTION WITH THE PUBLIC UTILITY GRID

When MMG operate in grid-connected mode, the distribution system operator decides the amount of energy to buy or sell from the utility grid, with an integration of smart retail pricing from the electricity operator with different hourly price during day. The interaction with the external grid is modeled as follows

$$C_i^{grid}(k) = \begin{cases} \eta_{sell} \lambda_{rt}(k) P_i^{grid}(k) \Delta t, & \text{if } P_i^{grid}(k) \leq 0 \\ \eta_{buy} \lambda_{rt}(k) P_i^{grid}(k) \Delta t, & \text{otherwise} \end{cases} \quad (1)$$

with

$$\underline{P}_i^{grid}(k) \leq P_i^{grid}(k) \leq \bar{P}_i^{grid}(k) \quad (2)$$

where  $\lambda_{rt}$  represent the retail price from the main utility grid electricity market at time interval  $k$ ,  $n$  represent the network losses.

### B. ENERGY STORAGE SYSTEM

The storage devices can be used to compensate imbalances arising from uncontrollable loads and generators. Thus, it is a critical part of each MG system which guarantees energy supply, and the smooth intermittent of renewable energy. To define the state of storage at a time interval  $(k - th)$  sampling time. Therefore, similar to [42], we denote  $E_i^b(k)$  as the energy stored in batteries of microgrid  $i$ , with the following associated discrete dynamic model as follows

$$E_i^b(k+1) = E_i^b(k) + \eta_i P_i^b(k) \quad (3)$$

where

$$\eta_i = \begin{cases} \eta^{chr}, & P_i^b(k) > 0 \\ 1/\eta^{dch}, & P_i^b(k) < 0 \end{cases} \quad (4)$$

where  $P_i^b(k) > 0$  and  $P_i^b(k) < 0$  means the battery charging and discharging, respectively.  $\eta_i$  is the coefficient efficiency of charging/discharging process. In order to extend the life-span At each time interval  $k$ , the state of charge (SOC) is controlled within the optimal range  $[\underline{E}_i^{dch}, \bar{E}_i^{chr}]$  defined minimum and maximum charge/discharge limits respectively. The boundaries represented in (5) and (6) are the constraints on the state of charge and the power of the storage battery to avoid the battery over-charge or over-discharge without penalizing the surplus energy trading between MMG.

$$\underline{E}_i^{dch} \leq E_i^b(k) \leq \bar{E}_i^{chr} \quad (5)$$

$$\underline{P}_i^b \leq P_i^b(k) \leq \bar{P}_i^b \quad (6)$$

The operation and maintenance (O&M) cost of the battery [43], at each time interval. It is introduced as follows.

$$C_i^b(k) = [2z_i^b(k) - P_i^b(k)] OM_b \Delta t \quad (7)$$

where the positive value  $z_i^b = \delta^b(k) P_i^b(k)$ ,  $\delta(k)$  is a binary value (1 or 0) for charging /discharging of the storage unit status.  $z_i^b$  is added to improve the efficiency and flexibility of battery operation within the range  $[\underline{P}_i^b, \bar{P}_i^b]$ .

### C. LOAD DEMAND MODEL

We consider two types of loads. First, critical loads: defined as  $P_i^{CL}$  is the load that must be satisfied with the demand-supply along the prediction horizon. The second type is the controllable load denoted by  $P_i^{SL}$ , which is the flexible load that can be controlled and scheduled later. For instance, heating system or charging an electric vehicle. The total load defined by  $P_i^L$  representing the sum of the two loads categories, subject to the following constraints

$$P_i^L(k) = P_i^{CL}(k) + P_i^{SL}(k) \quad (8)$$

$$\underline{P}_i^L(k) \leq P_i^L(k) \leq \bar{P}_i^L(k) \quad (9)$$



with

$$0 \leq P_i^{SL}(k) \leq \bar{P}_i^{SL}, \quad \forall i \in M \quad (10)$$

where  $\underline{P}_i^L$  and  $\bar{P}_i^L$  in (9) corresponding to the minimum and maximum active power, respectively.

#### D. DG OPERATING CONDITION

In our study, the DG unit employed as a dispatchable power that can be scheduled over a specific horizon with efficiency. The main reason of using DG as a distributed generation due to the fuel availability and transportation facilities compare to gas [44], power flow output limit of the generator as follows

$$\delta_i^{DG} \underline{P}_i^{DG}(k) \leq P_i^{DG}(k) \leq \delta_i^{DG} \bar{P}_i^{DG}(k) \quad (11)$$

where

$$\delta_i^{DG} = \begin{cases} 1, & P_i^{DG}(k) > 0 \\ 0, & P_i^{DG}(k) = 0 \end{cases} \quad (ON/OFF \text{ switch}) \quad (12)$$

The following constraints are used for maintaining the minimum amount of time of the generator unit state, which must be kept ON/OFF with minimum up/downtime constraints as follows

$$\begin{aligned} \delta_i^{DG}(k) - \delta_i^{DG}(k-1) &\leq \delta_i^{DG}(\tau), \quad (OFF/ON) \\ \delta_i^{DG}(k-1) - \delta_i^{DG}(k) &\leq 1 - \delta_i^{DG}(\tau), \quad (ON/OFF) \end{aligned} \quad (13)$$

where  $\tau$  is an auxiliary variable, For example, at the time step  $k$ , with  $\delta_i^{DG}(k-1) = 0$ , meaning that DG unit was OFF in previous sampling time. The operation cost on fuel consumption [45] during an interval time can be expressed as follows

$$C^{DG}(P_i^{DG}(k)) = (a_i(P_i^{DG}(k))^2 + b_i P_i^{DG}(k) + c_i) \Delta t \quad (14)$$

In the quadratic polynomial function above, parameters (a,b) and (c) a the cost coefficients of the DG power output at time  $k$ .

#### E. RENEWABLE ENERGY

In this paper, solar energy form PV power plant installed on the rooftop of the green energy laboratory mentioned in previous section. However, the following constraint imposed on the total power generated from renewable sources.

$$\underline{P}_i^{RES} \leq P_{i,k}^{RES} \leq \bar{P}_i^{RES} \quad (15)$$

where  $\underline{P}_i^{RES}$  and  $\bar{P}_i^{RES}$  denote the minimum and maximum of power production, which is limited by total capacity of electrical distribution lines. Since PV are considered to have high volatility due to natural processes such as storms and clouds. Thus, we assume that RESs in each MG operate between its power output limits.

#### F. POWER BALANCE

Suppose there are a total of  $M$  microgrids in the studied cooperative energy system, which is demonstrated in Fig. 2. At each time interval  $k$ , the main objective for the cooperative MMG-EMS is to guarantee the power balance of supply-demands. Thus, the following equality represents the balance between energy consumption and production by means of energy mismatch as follows

$$\begin{aligned} P_i^S(k) &= P_i^{DG}(k) + E_i^{dch}(k) - E_i^{ch}(k) \\ &\quad + P_{ij}^{surp}(k) + P_i^{grid}(k) - P_i^{SL}(k) \end{aligned} \quad (16)$$

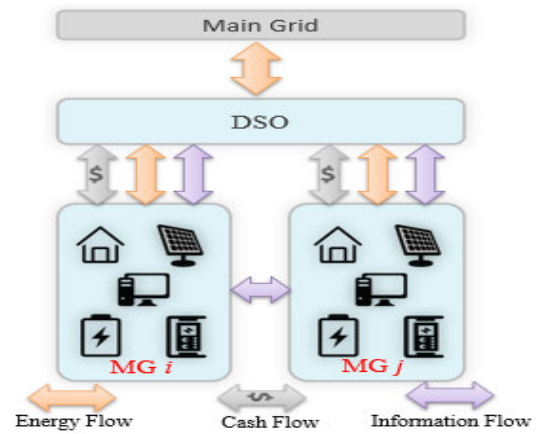


FIGURE 2. Cooperative energy management scheme.

with

$$P_i^S = P_i^{CL}(k) - P_i^{RES}(k) \quad (17)$$

$$P_{ij}^{surp}(k) = \sum_{j \neq i}^m a_{ij} P_j^S(k) \quad (18)$$

With  $P_i^S(k)$  denote the power mismatch,  $P_i^{grid}(k)$  in (16) represent the energy purchased from the main grid by the DSO. In addition, we added the condition on the surplus power  $P_{ij}^{surp}(k) \geq 0$  to maximize the use of renewable energy.

#### IV. RETAIL ELECTRICITY PRICE PREDICTION BASED ON THE OR-ELM LEARNING MODEL

In this section, a Robust regression algorithm based on OR-ELM is formulated. The robust regression model is then evaluated with other machine learning algorithms for EPF. The training and testing performance are based on historical LMP data from the ISO New England market. First, a brief description of the ELM framework is proposed.

##### A. EXTREME LEARNING MACHINE

The ELM consider as a single-hidden feed-forward neural network, Fig. 3 illustrates the SLFN regression model with  $L$  hidden nodes and  $g(x)$  activation function for  $M$  arbitrary samples  $(x_i, t_i) \in \mathbb{R}^n \times \mathbb{R}^m$ , where  $x_i[x_{i1}, x_{i2}, \dots, x_{im}]$  and  $t_i = [t_{i1} + t_{i2}, \dots, t_{im}]$ , the advantage of ELM-SLFN is the allocation of the weights vectors and thresholds between the

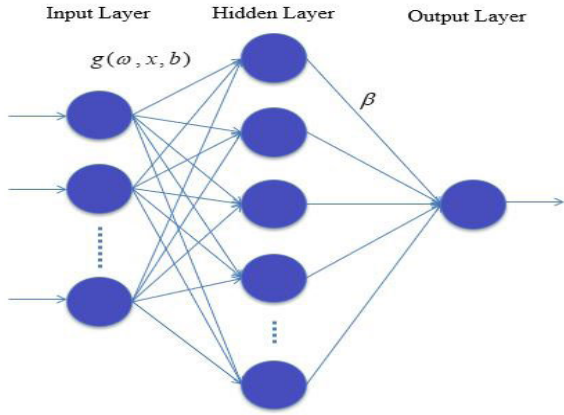


FIGURE 3. ELM-SLFN structure.

input layer and hidden layer randomly, without changes of the model parameters through the entire learning process. Thus, it can complete the training process extremely fast [46].

The main parameters of ELM approach are modelled as follow

$$f_N = \sum_{i=1}^N \beta_i g(\omega_i x_j + b_i) = y_j \quad (19)$$

where  $\omega_i$  is the weight vector that connects the  $i^{th}$  hidden neurons and input neurons,  $\beta_i$  is the weight vector that connects the  $i^{th}$  hidden neuron and output neuron, both weights vectors  $\omega_i$  and  $\beta_i$  are represented as  $[\omega_{i1}, \omega_{i2}, \dots, \omega_{in}]^T$  and  $[\beta_{i1}, \beta_{i2}, \dots, \beta_{im}]^T$  respectively  $b_i$  is the threshold of  $i^{th}$  hidden neurons, and  $\omega_i \times x_j$  represent the inner product  $\omega_i$  and  $x_j$ . In order to find  $\beta$  vector a Least Square Error (LSE) is applied, the solution can be expressed as follows:

$$\beta = H^\dagger Y = (H^T H)^{-1} Y \quad (20)$$

$$H = (\omega_1, \dots, \omega_N, b_1, \dots, b_N, \dots, x_1, \dots, x_N) \\ = \begin{bmatrix} g(\omega_1 x_1 + b_1) & \dots & g(\omega_N x_1 + b_N) \\ \vdots & \dots & \vdots \\ g(\omega_1 x_N + b_1) & \dots & g(\omega_N x_N + b_N) \end{bmatrix}_{N \times M} \quad (21)$$

$$\beta = \begin{bmatrix} \beta_1^T \\ \vdots \\ \beta_N^T \end{bmatrix}_{N \times M}, \quad Y = \begin{bmatrix} \omega_1^T \\ \vdots \\ \omega_M^T \end{bmatrix}_{M \times m} \quad (22)$$

where  $H$  is the output matrix of the  $L$  hidden layer. The output weight is obtained by solving the following minimization.

$$\min_{\beta} \|H\beta - Y\| \quad (23)$$

The optimal solution of the above minimization is given as

$$\hat{\beta} = H^\dagger Y \quad (24)$$

where  $H^\dagger$  refer to the Moore-Penrose generalized inverse matrix of  $H$ .

Nevertheless, the presence of the outliers may result in an unstable or unreliable ELM model. Therefore an improved

ELM algorithm is introduced in [47] with two stages, first the ELM regularization by adding a regularized parameter  $C$  and the second stage introduces a new solution based on the training errors minimization. In the following, the principle of the improved Outlier-Robust ELM is presented.

### B. OUTLIER ROBUST ELM

To minimize the ELM training error and avoid the model overfitting and improve the regression accuracy, a regularized ELM have been introduced in [48] for regression problems such as the over-fitting problems, which affect the prediction accuracy. Therefore, introducing a regularization parameter  $C$  is necessary for better performance. Consequently, the output  $\beta$  in (20) is replaced by an alternative solution with less computational time and more regression performance accuracy as follows

$$\hat{\beta} = H^T (H^T + \frac{1}{C})^{-1} Y \quad (25)$$

However, to improve the regression robustness, a minimization of the training errors and the output weights will be updated in every iteration. Accordingly, the novel robust ELM approach was proposed in [47] to minimize the outliers that occurred. The following are the mathematical model of the OR-ELM is used instead of the function (23) is given as

$$\min_{\beta} \|e\|_1 + \frac{1}{C} \|\beta\|_2^2 \text{ subject to } Y - H\beta = e \quad (26)$$

where  $e$  denotes the training error, with  $e = [e_1, e_2, \dots, e_N]^T$   $C$  is the regularization parameter. The above objective function in (26) is a constrained convex optimization, which can be solved by the augmented Lagrange multiplier method using the following iterative scheme:

$$\begin{cases} \beta_{k+1} = \arg \min_{\beta} L_{\mu}(e_k, \beta, \rho_k) \\ e_{k+1} = \arg \min_e L_{\mu}(e, \beta_{k+1}, \rho_k) \\ \rho_{k+1} = \rho_k + \mu(Y - H\beta_{k+1} - e_{k+1}) \end{cases} \quad (27)$$

where  $\rho_k$  is the vector of the Lagrange multipliers.  $\mu$  is a penalty parameter. Then, the solution for the weight output  $\beta_{k+1}$  and  $e_{k+1}$  are given by

$$\begin{cases} \beta_{k+1} = (H^T H + \frac{2}{k\mu I})^{-1} H^T (Y - e_k + \frac{\rho_k}{\mu}) \\ e_{k+1} = \text{shrink}(Y - H\beta_{k+1} + \frac{\rho_k}{\mu}, \frac{1}{\mu}) \end{cases} \quad (28)$$

During the test stage, a test data  $x$  is stored by the following equation

$$F(x) = h(x)\beta \quad (29)$$

In the Algorithm (1) a detailed steps of the Outlier Robust ELM.

**Algorithm 1** OR-ELM

---

```

1: procedure ORELM learning model(1)
2: input: Set a training data for  $M$  arbitrary samples  $(x_i, t_i)$ 
   with  $(g(x))$  activation function,  $(L)$  hidden layer node,
    $C$  a constant parameter, and the maximum number of
   iteration  $MaxIter$ .
3: Randomly generate hidden node parameters  $(w_i, b_i)$ 
4: Obtain hidden layer output matrix  $H$ 
5: The Parameters setting and initialization
6:   for  $k = 1$  to  $MaxIter$  do
7:      $\beta_{k+1} = \arg \min_{\beta} L_{\mu}(e_k, \beta, \rho_k)$ 
8:      $e_{k+1} = \arg \min_e L_{\mu}(e, \beta_{k+1}, \rho_k)$ 
9:      $\rho_{k+1} = \rho_k + \mu(Y - H\beta_{k+1} - e_{k+1})$ 
10:     $k \leftarrow k + 1$ 
11:   end for
12: Return and save the testing results by (29)
13: end procedure

```

---

**C. EXPERIMENT EVALUATION OF OR-ELM MODEL FOR ELECTRICITY PRICE MARKET FOR ONE WEEK AHEAD**

In this section, an experimental evaluation is proposed of the OR-ELM learning algorithm for electricity retail price prediction based on historical LMP dataset [49] from ISO New England. The data is collected with 1 hour time interval during day from January 1 to December 31 in 2019, which is illustrated in Fig. 4. At first phase, data pre-processing has been established to classify the training and testing dataset. The training data is formed by 672 samples from last seven days of four months; August, November, February, and May, as representatives of summer, autumn, winter, and spring seasons, respectively. The reason of choosing seasonal data profile, to get an accurate electricity price prediction, since the drop or rise of temperature and the change of weather parameters have a decisive impact on the electricity consumption [50]. For instance, the extreme temperature can increase demand for heating and cooling. In the other hand, the weekly average samples with 168 samples is used for testing validation from the remaining dataset which not have been involved

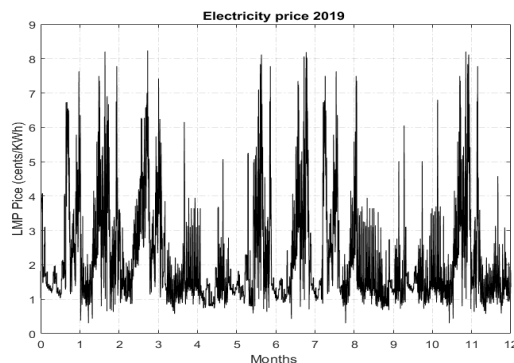


**FIGURE 4.** Electricity price from the ISO New England market (January 1-December 31, 2019).

in the training development. The effectiveness of OR-ELM and other comparative methods for the LMP prediction is evaluated with the commonly metric errors measurements such as  $R^2$ , MAE, and MAPE, which can be calculated as follows

$$R^2 = 1 - \frac{\sum_{i=1}^n (p_i - \hat{p}_i)^2}{\sum_{i=1}^n (p_i - \bar{p})^2} \quad (30)$$

$$MAE = \frac{1}{n} \sum_{i=1}^n |\hat{p}_i - p_i| \quad (31)$$

MAPE provide the metric errors in terms of percentage and is given by the following formulation

$$MAPE = \frac{100}{n} \sum_{i=1}^n \left| \frac{\hat{p}_i - p_i}{p_i} \right| \quad (32)$$

where  $p_i$  and  $\hat{p}_i$  indicate the actual electricity price and the predicted value, respectively.  $n$  denotes the number of training samples. The RMSE standard metric is employed to evaluate the accuracy of the prediction results, the associated RMSE is defined by the following formulation

$$RMSE = \sqrt{\frac{1}{n} \sum_{i=1}^n (\hat{p}_i - p_i)^2} \quad (33)$$

The LMP hourly retail price selected in our modeling is expressed by  $\lambda_t, t = 1, \dots, T$ , and the input vector of the OR-ELM is  $[\lambda_1, \lambda_2, \dots, \lambda_T]^T$ , and the output matrix is expressed as  $[F_1, F_2, \dots, F_M]^T$  with  $F$  is the forecasted electricity price for  $M$  samples. The simulation horizon is denoted by  $h$  step-ahead for OR-ELM, SVR, and ANN. Finally, all  $F$  values are summed to obtained the  $h$  step-ahead electricity forecast results. For the OR-ELM model parameters: The number of hidden neuron  $H = 150$ ,  $C = 1.75$ , and sigmoid kernel as an activation function.

Fig 5 illustrates a 10-fold Cross-Validation (CV) procedure for RMSE, such as a total data with 840 dataset is sampled randomly with fraction of 672 samples for training and 168 for testing data from the same dataset, the CV procedure is then, repeated 10 times (10-fold), using different patterns for training and validation. It is obvious from the plot that the optimum RMSE value is located between the range of 6 and 8 cross validation for the three models. For example, the mean values of RMSE are 1.81, 2.1, and 2.4 for the OR-ELM, SVR, and ANN, respectively, therefore, it validate our dataset processing, and display the efficiency of the proposed learning algorithm.

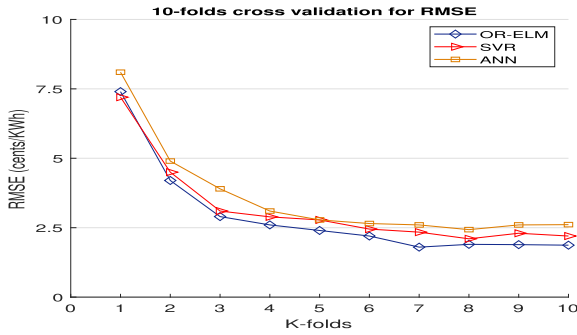
Fig. 6 shows the training results for ANN, SVR, and OR-ELM, respectively. It can be seen that the regression analysis for SVR and OR-ELM are quite similar for error metric ( $R^2$ ) evaluation with 0.9173 for SVR and 0.9568 for OR-ELM while for the ANN model is 0.8893, the OR-ELM minimize the errors by deleting the outliers in the training stage. Table 1 and Table 2 present training and testing results based on the

**TABLE 1.** Training performance with error metrics evaluation and computational time.

Forecast model	$R^2$	MAE	MAPE (%)	Time (s)
ANN	0.8893	5.91	6.29	0.9158
SVR	0.9173	1.12	4.17	4.8623
OR-ELM	0.9568	0.93	2.05	0.8023

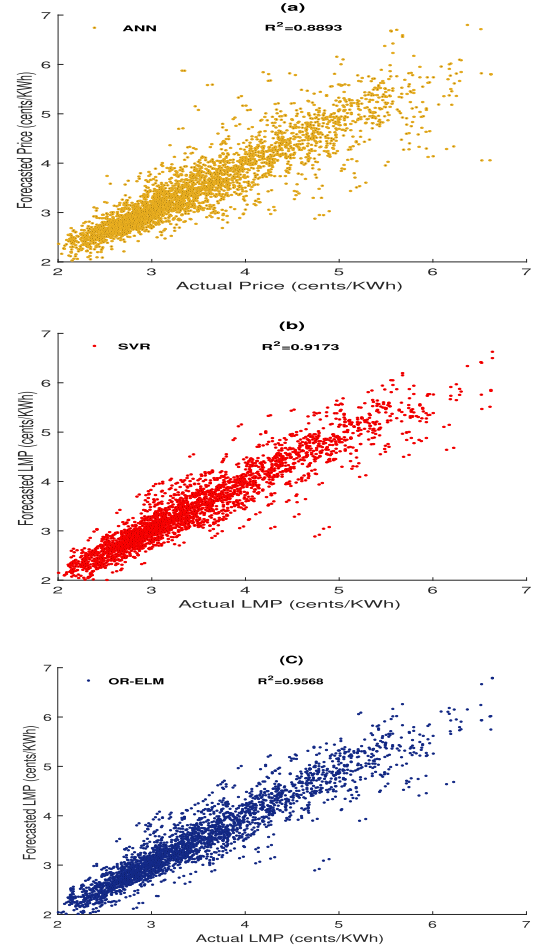
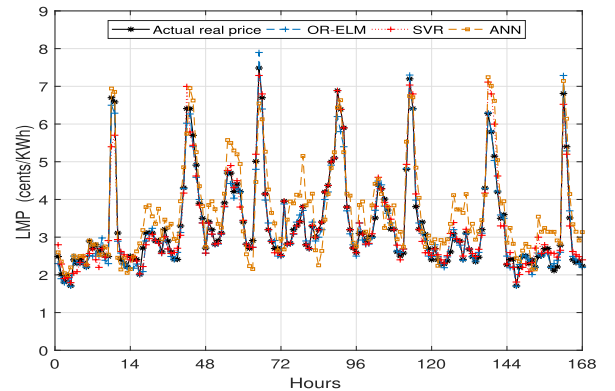
**TABLE 2.** Testing performance with error metrics evaluation and computational time.

Forecast model	$R^2$	MAE	MAPE (%)	Time(s)
ANN	0.8741	7.91	8.47	0.0650
SVR	0.9083	2.33	6.88	0.9031
OR-ELM	0.9379	1.87	4.92	0.0886

**FIGURE 5.** Plot of the 10-folds cross validation by RMSE with OR-ELM, SVR, and ANN.

error metrics  $R^2$ , MAE, MAPE, and the computational time. It is obvious that the proposed OR-ELM algorithm shows better performance and less errors with a faster computing time in the training and testing. For example, in training stage OR-ELM has 0.8023 computing time, however, for the ANN and SVR algorithms are 0.9158 and 4.8623 respectively. Similarly, in the testing stage. For example, the MAPE is 8.47, 6.88, and 4.92 for ANN, SVR, and OR-ELM. Also, in Table 2 the  $R^2$  results is 0.8741, 0.9083 and 0.9379 for or ANN, SVR, and OR-ELM respectively.

In addition, Fig 7 demonstrates the forecasting performance of ANN, SVR and OR-ELM based on the testing weekly average pricing dataset. It could be observed that the overall OR-ELM has a better performance for tracking real price curve. The findings results show that the OR-ELM prediction model is faster and more accurate than SVR and ANN for electricity price forecasting therefore, it is suitable to provide an accurate electricity price to the DSO to solve the energy dispatch problem for the cooperative MMG network. From the above evaluation results, it's evident that the OR-ELM method efficiency is superior to the SVR model in terms of computing time and accuracy for electricity price forecasting. Note that the main idea from this comparison is to justify using the robust ELM algorithm among similar regression approaches. Therefore, the proposed regression model is suitable for moving horizon optimization same as the robust distributed MPC Framework.

**FIGURE 6.** Scatter plots of the forecasted and actual electricity price LMP using the training models: ANN (a), SVR (b) and OR-ELM (c).**FIGURE 7.** Forecasted retail electricity market with ANN, SVR and OR-ELM with comparison to the average weekly price.

## V. ROBUST DATA PREDICTIVE CONTROL FOR MMG ENERGY MANAGEMENT SYSTEM

In this section, the two layers of cooperative optimization problems are formulated. First, a cooperative MMG energy planing for one day ahead is formulated, taking into consideration the retail electricity pricing forecasted by the OR-ELM



to reduce the total operating cost. As for the second layer each local controller executes the optimal trajectory.

#### A. MMG DYNAMIC MODEL

The main objective of our study is to achieve an efficient economic energy dispatch for the MMG systems while reducing the operation cost, using a hierarchical dual-level optimal control based on cooperative distributed MPC. The following dynamic model for the  $i$ th MMG system is introduced as

$$\begin{aligned} x_i(k+1|k) &= a_i x_i(k|k) + b_i u_i(k|k) \\ y_i(k|k) &= c_i u_i(k|k) \end{aligned} \quad (34)$$

where in the dynamic model (34), the system state, inputs and output are given as follow

$$\begin{aligned} x_i(k|k) &= [E_i^b(k|k)], \\ u_i(k|k) &= [P_i^{SL}(k|k), P_i^{grid}(k|k), P_i^{DG}(k|k), \\ &\quad E_i^{ch}(k|k), E_i^{dch}(k|k)] \\ y_i(k|k) &= [P_i^S(k|k)] \end{aligned}$$

Note that throughout this thesis, the double subscripts notation  $(k+l)$ ,  $l \geq 0$  describes the prediction of the states and inputs with  $l$  steps ahead from time interval  $k$ . As a result, we have  $x_i(k+l|k) \in \Phi^{n_i}$  and  $u_i(k+l|k) \in \Omega_i$ , where  $\Omega_i \subset \Phi^{m_i}$  which is the admissible controls for the  $i$ th subsystems. Further, in our optimization, the time horizon is one day  $N = 24$  for energy dispatch for 24 h ahead. In following the finite horizon prediction of states and inputs trajectories for distributed MPC as follows.

$$\begin{aligned} x_i(k) &= [x_i(k+1|k), x_i(k+2|k), \dots, x_i(k+N|k)]^T \\ u_i(k) &= [u_i(k|k), u_i(k+1|k), \dots, u_i(k+N-1|k)]^T \end{aligned}$$

#### B. FIRST LAYER OPTIMIZATION: DSO OPTIMAL ENERGY SCHEDULING

In the first level, the DSO will compute the electricity retail price with OR-ELM for a day ahead while based on historical data from wholesale market. Moreover, there also exists information exchange between different layers in both directions. For example, the states information from each local controller including the energy mismatch. Given that the demand may exceed the supply among the whole MMG system. Hence, the purchase electricity from utility grid is compulsory to maintain power balance. In the case of energy surplus availability, the trading energy between MMG will be considered. The upper layer aims to plan the optimal set-points for each microgrid so that the energy dispatch can be balanced by scheduling the distributed energy resources such as battery, DGs units, and the energy surplus. The following objective function is formulated to guarantee cooperative energy trading and scheduling between DSO and MGs systems as follows

$$\min \sum_{l=1}^N \sum_{i=1}^M \xi_{i1} ((E_i^{chr}(k+l|k) - (E_i^{dch}(k+l|k)))$$

$$+ \xi_{i2} \lambda_{i,r} P_i^{grid}(k+l|k) + \xi_{i3} C_i^{DG}(P_i^{DG}(k+l|k) + \xi_{i4} C_i^b(P_i^b(k+l|k)))$$

$$s.t. (1) - (16), (34)$$

$$\sum_i^M P_i^{CL}(k+l|k) \leq \sum_i^M P_i^{RES}(k+l|k) \quad (35)$$

where  $N$  denote the control horizon,  $\lambda_{i,r}$  is the retail computed with the OR-ELM algorithm for same period.  $\xi_i$  is the weighting factors with  $i = 1, 2, 3, 4$ . The first two terms are related to the battery charge/discharge operation, and the second cost is related to selling and purchasing energy from the main grid, whereas the third terms are related to the cost of the diesel generators units, and the last term related to the battery maintenance cost. To guarantee the critical load to be met at each time, we assume that the power on renewable energy superior or equal to the critical load

The DSO guarantees the demand-supply balance for each MG with optimal operating costs in term of purchasing energy from the main grid or using the power from the controllable generators. The optimal solution in (35) is  $\gamma_i^{ref}(k+l|k)$  and it can express as follows

$$\begin{aligned} \gamma_i^{ref}(k+l|k) &= E_i^{chr}(k+l|k) - E_i^{dch}(k+l|k) \\ &+ P_i^{surp}(k+l|k) + P_i^{DG}(k+l|k) + P_i^{grid}(k+l|k) \end{aligned} \quad (36)$$

The above set-point reference  $\gamma_i^{ref}$  will send to the second layer the local controller, and each MG will track this optimal trajectory. The problem formulation for the local controller is given in the following sub-section.

#### C. SECOND LAYER: LOCAL CONTROLLER ENERGY DISPATCH

The main objective is to achieve a global economic dispatch for the MMG system. Therefore, the following objective function for efficient energy dispatch by tracking the optimal energy scheduling  $\gamma_i^{ref}$  and minimizing the operating cost. Thus, the optimization  $J_i(u_i(k))$  is introduced as follows

$$\begin{aligned} J_i(u_i(k)) &= \min \sum_{l=1}^N \zeta_1 (P_i^L(k+l|k) - \gamma_i^{ref}(k+l|k))^2 \\ &+ \zeta_2 ((E_i^{chr}(k+l|k) - (E_i^{dch}(k+l|k)))^2 \end{aligned} \quad (37)$$

With  $\zeta_1, \zeta_2$  are weighting coefficients. The above objective represents the local controller optimization of each MG, such that each MG solve the above optimization by adjusting the total active loads, and reschedule the local battery for optimal charge/discharge operation at the LC-MG level.

#### D. ITERATIVE ALGORITHM FOR ROBUST DATA-PREDICTIVE CONTROL-ENERGY MANAGEMENT SYSTEM RDPC-EMS

In this stage, both optimizations for DSO and local controller have been designed. First, the OR-ELM regression model is used to obtain the forecasted electricity price for  $h$  horizon in our study 24 hours (one day ahead). Next, The DSO broadcasts the computed  $\gamma_i^{ref}(k+l|k)$  reference to each

local controller after solving the first energy management optimization. After that, in the second optimization cycle each local controller LC-MG receive the optimal solution and solve its local objective.

#### Algorithm 2 RDPC-EMS

```

1: procedure Hierarchical Predictive control(2)
2: Initialization: set the initial values for each ith
   MG  $E_i^{chr}(0), E_i^{dch}(0), P_i^L(0), P_i^{SL}(0)P_i^{RES}(0)$  with
    $i = 1, 2 \dots M$ 
3: Get the forecasted electricity retail price  $\lambda_r$  computed by
   the OR-ELM algorithm (1).
4: for  $k = 1$  do
5:   Compute energy mismatch  $P_i^S$  from each MG
6:   Broadcast energy mismatch to the network
7:   Solve the optimization (35) at the first-level DSO
8:   Until convergence
9:   Receive optimal solution  $\gamma_i^{ref}(k + l|k)$ 
10:  Solve second layer optimization (37) at LC-MG
11:  Until convergence
12:  Implement first optimal control solution.
13:  Set new iteration  $k = k + 1$ , and go to step 4
14: end for
15: end procedure

```

#### E. STABILITY AND CONVERGENCE OF THE PROPOSED FRAMEWORK

From the definition of cooperative DMPC [51], the time dependence of states and inputs vectors trajectories are dropped in the DMPC framework in (37), such as  $J_i(u_i) \leftarrow J_i(u_i(k))$  and  $u_i \leftarrow u_i(k), x_i \leftarrow x_i(k)$  with  $i = 1, \dots, m$ . Thus, the cooperation based cost function  $J(\cdot)$  after  $p$  iterations for the wide-system impact of local control actions as follows

$$J(u_1^p, u_2^p, \dots, u_m^p) = \sum_{i=1}^m \omega_i J_i(u_1^p, u_2^p, \dots, u_m^p) \quad (38)$$

With  $\omega_i > 0$ , if  $J(u_i)$  is convex over the set admissible  $\Omega_i$  for  $\forall_i = 1, 2, \dots, m$ . Then, the sequence of cost functions objectives  $J(u_1^p, u_2^p, \dots, u_m^p)$  generated by the algorithm 2 is non-increasing with the iteration number  $p$ .

In the light from the proofs of Lemma 1 and Lemma 2 in [52], the following proof is given. Let  $u_i^{*(p)}$  denote the optimal solution, for the  $i$ -th subsystems with  $i = 1, \dots, m$  we have

$$\begin{aligned} J(u_i^{p-1}, \dots, u_{i-1}^{p-1}, u_1^{*(p)}, u_{i+1}^{p-1}, \dots, u_m^{p-1}) \\ \leq J(u_1^{p-1}, \dots, u_{i-1}^{p-1}, \dots, u_{i+1}^{(p)}, \dots, u_m^{p-1}) \end{aligned} \quad (39)$$

Hence, from (38) we have

$$\begin{aligned} J(u_i^{p-1}, \dots, u_{i-1}^{p-1}, u_1^{*(p)}, u_{i+1}^{p-1}, \dots, u_m^{p-1}) \\ = J(\omega_1 u_i^{*(p)} + (1 - \omega_1) u_1^{p-1}, \dots, \omega_m u_m^{*(p)} + (1 - \omega_m) u_m^{p-1}) \end{aligned} \quad (40)$$

by convexity of  $J(\cdot)$

$$\begin{aligned} &\leq \sum_{i=1}^m \omega_i J_i(u_1^{p-1}, \dots, u_{i-1}^{p-1}, u_i^{*(p)}, u_{i+1}^{p-1}, \dots, u_m^{p-1}) \\ &\leq \sum_{i=1}^m \omega_i J_i(u_1^{p-1}, \dots, u_{i-1}^{p-1}, u_i^{p-1}, u_{i+1}^{p-1}, \dots, u_m^{p-1}) \\ &= J_i(u_1^{p-1}, u_2^{p-1}, \dots, u_m^{p-1}) \end{aligned} \quad (41)$$

In which the equality is obtained with  $u_i^p = u_i^{p-1}$ . Therefore, this results assures non-increasing. Thus, we have  $J_i(u_i) > 0, \forall_i = 1, 2, \dots, m$ , using the convexity of  $\Omega_i = \Omega_1, \Omega_2, \dots, \Omega_m$ , then,  $J_i(u_i)$  in DMPC optimization (37) is convex and bounded below which assures convergence of the sequence of cost functions with the iteration number. The detailed proof is similar to Lemma 1 in [52]. For simplicity, the full proof is omitted.

#### VI. SIMULATION AND ANALYSIS

The MMG systems considered in the simulations are shown in Fig. 8, each MG compromise of PV, ESS, load demand, DG unit, and each LC-MG is connected to DSO. The PV power from Green Energy Laboratory-Shanghai Jiao tong university, and the demand load from the open-source [53]. The LMP electricity pricing was used from ISO New England online data to forecast a day-ahead retail electricity price. The cooperative MMG community is comprising with similar DERs units.

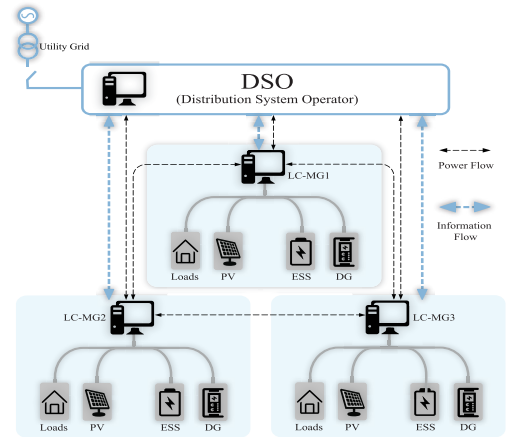


FIGURE 8. Illustration of the studied MMG.

#### A. SIMULATION SET-UP

Table 3 presents the batteries initial parameters. The DG power limit  $\bar{P}_i^{DG} = 10$ , with  $a_i = 0.06, b_i = 0.4$ ,

TABLE 3. Parameter for storage energy systems.

MMGs	$\bar{E}_i^{chr}$	$\bar{E}_i^{disch}$	$\eta_i^{chr}$	$\eta_i^{disch}$	$E_i(0)$
MG1	25	0.5	0.60	0.75	12
MG2	20	0.5	0.25	0.40	10
MG3	15	0.5	0.50	0.65	15

$c_i = 1.05$  are the fuel cost parameters, and fuel cost for DG is 6 cent/KWh. Let the weights coefficients  $\xi_1 = 0.2$ ,  $\xi_2 = 0.4$ ,  $\xi_3 = 0.5$ ,  $\xi_4 = 0.5$  and  $\zeta_{i1} = 0.7$ ,  $\zeta_{i2} = 0.5$ . The energy storage O&M cost is 4 cent/KWh and self-discharge rate is 0.5 kW. The hourly average retail price data set for the same data used the OR-ELM model previously to forecast 1 hour ahead LMP electricity price and testing with real measured data from section IV.

Fig. 9 shows the forecast retail electricity price and average electricity price for one day ahead from the OR-ELM regression. The dataset remains unchanged similar as section IV. However, the model is set to forecast electricity prices for 24 hours. Also, we assumed that the same retail electricity price is associated to the whole MMG system. Fig 10 illustrates the actual load and PV power generation for each MG. It is obvious that there is an unbalance between demand-supply, especially for MG1 as the renewable energy is less than demand load from along the 24 h. On the other hand, MG2 and MG3 have surplus PV energy production in some time slots during 24. For instance, in MG2, from 10 am to 4 pm, the energy from PV was more than the load demand. To validate the performance of the proposed energy scheduling framework, the following two cases are considered:

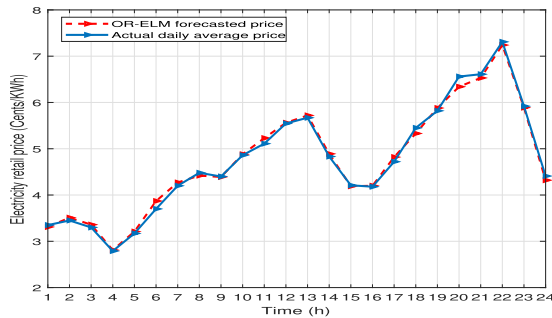


FIGURE 9. Forecasted electricity price using OR-ELM.

- *Case Study 1 (CS1)*: Cooperative MMG connected to the higher level DSO, sharing same electrical bus and exchange energy and sharing information between each other.
- *Case Study 2 (CS2)*: Non-cooperative MMG each MG connected to the higher level DSO and operated independently without sharing energy between each other.

## B. RESULTS AND DISCUSSION

Fig. 11 demonstrates efficient results of energy dispatch based on our proposed iterative algorithm using cooperative scenario (CS1). It can be seen that the energy scheduling for one day ahead shows an efficient energy dispatch using controllable distributed energy resources DER, such as diesel generator DG and energy storage system ESS, to supply the demand load with the necessary energy. Moreover, the cooperative MMG exchange surplus energy between each other. For instance, MG1 receives surplus energy from 10 am to 3 pm from nearby MG. Similarly, MG3 used a part of the surplus energy from MG2. Simultaneously, the retail electricity

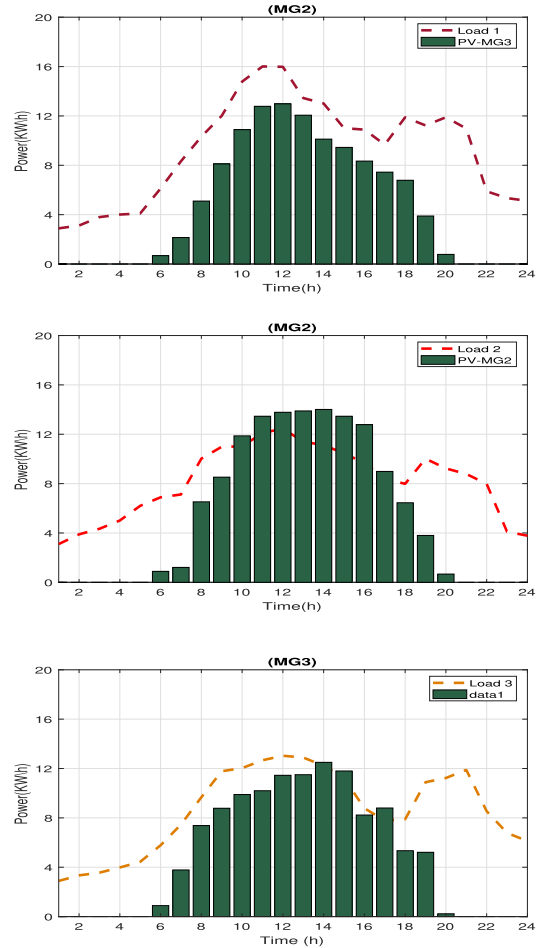
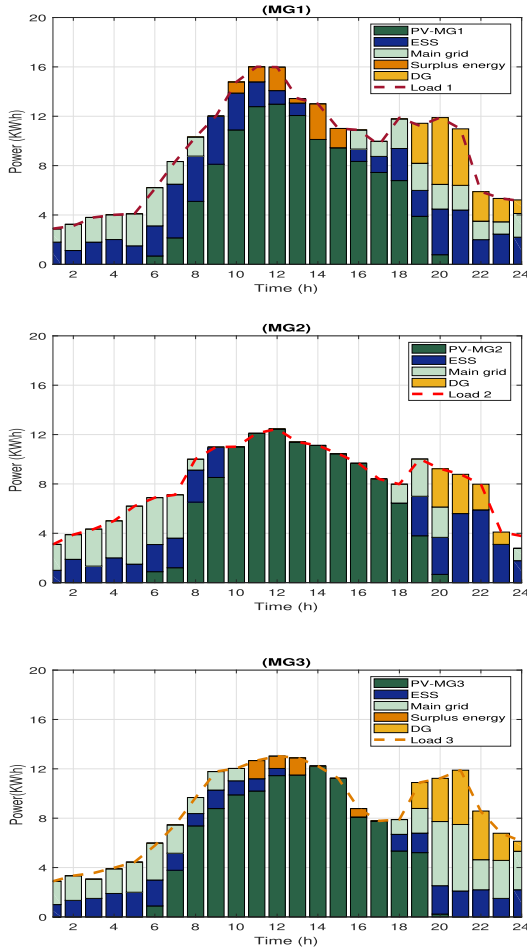


FIGURE 10. Profile of load demand and PV power generation for each microgrid.

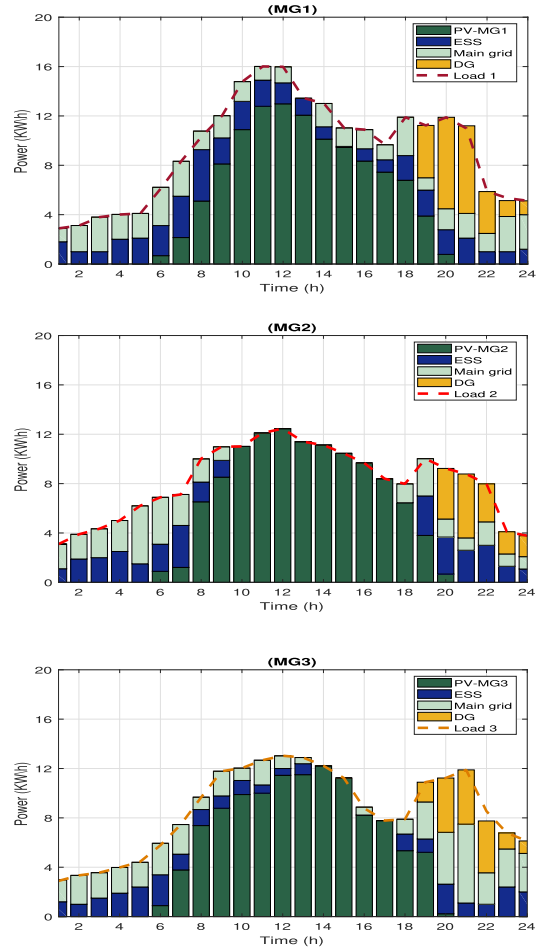
price, as shown in 9, was higher for the same period. On the other side, MG2 and MG3 open the DG energy backup from 8 pm to 12 am and 6 pm to midnight, respectively. As from fig 10 in the same time slot, the retail electricity price is higher than the cost of running the DG units.

Fig. 12 exhibits the energy dispatch results using a non-cooperative scenario (CS2). The results of energy scheduling for each MG operated independently indicates that without energy surplus, the MMG system tends to buy energy from the main grid to fill the gap between demand and supply. For example, MG1 purchased electricity from the main grid from 10 am to 3 pm with a high retail price, while in the cooperative case, it used the energy surplus shared by other MG2. Also, we observe that each MG tends to purchase energy from the main grid while charging their batteries. This behavior from local controllers after receiving the optimal scheduling from DSO is to reduce operation cost and save energy for future use. Moreover, to validate the advantage of the cooperative scenario (CS1).

Fig. 13 displays the state of charge for both cases of studies as. The positive values correspond to battery charging, while the negative ones denote the discharging. In both scenarios,



**FIGURE 11.** Energy dispatch and scheduling of each MG with the cooperative scenario (CS1).



**FIGURE 12.** Energy dispatch and scheduling of each MG with the non-cooperative scenario (CS2).

batteries assure the smooth intermittent of the renewable power for each MG. Furthermore, the storage systems operation is affected by the following three parameters: the initial capacity of each MG presented in Table 3, the constraints (5) and (6) and the optimal energy scheduling from the DSO upper layer. For instance, The MG2 charge its local battery during the availability of the energy surplus. However, we can

see that the charging is more important in the non-cooperative period following by a discharge to reduce the operation costs during the peak period where the electricity price is higher from period 7 pm to 11 pm. Meanwhile, MG2 and MG3 discharge partly their local batteries to compensate for the energy mismatch.

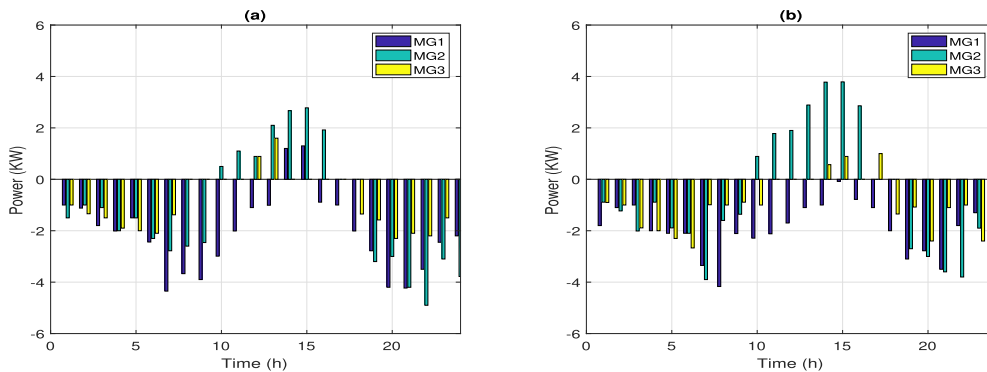


**FIGURE 13.** Profile of the state of the batteries charge/discharge in case of study (SC1) figure (a), and case of study (SC2) figure (b).



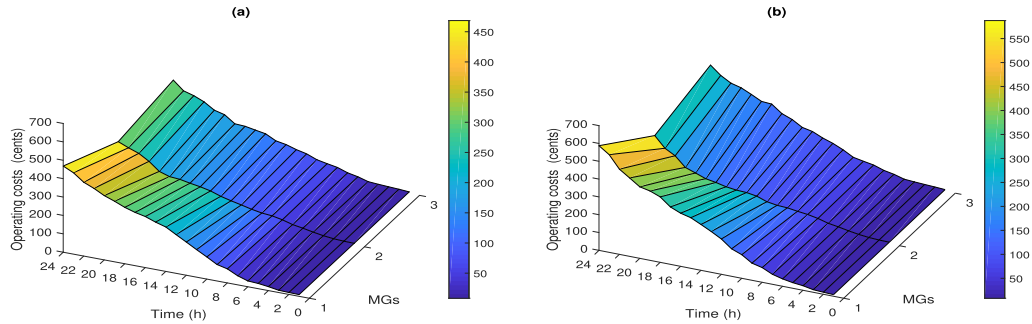


**FIGURE 14.** Total operating costs in cooperative case of study (SC1) figure (a), and non-cooperative case of study (SC2) figure (b).

Fig. 14 shows the total operating costs at each time interval  $k$  in the two case studies based on the proposed optimization, which the total operating costs is the sum of all the previous costs values. For example, the operating costs at 8 am, represents the sum of the previous 7 hours operating costs plus 1 hour costs value. The results show lower operating costs from 1:00 am to 7:00 am due to the minimal demand on the user's electricity. However, the operating costs increase dramatically in the day-time because of the rise of demand and the high electricity price in the peak hours 4:00 pm to 11:00 pm. The outstanding reduction of the operating costs in the cooperative scenarios optimization, mostly because of the use of surplus energy. For instance, the total operating cost for MG 1 is 468.5 (cents) with the cooperative scenario, While in the non-cooperative optimization is 587.4 (cents). The operating cost in non-cooperative is higher with more than 15%, in MG3 total operating cost increased from 376 (cents) if the first scenario to 450 (cents). In contrast, it remains almost the same in MG 2 due to sufficient PV energy. The difference in both scenarios can be explained by the extensive use of DG units and purchasing electricity from the main grid. The previous results proved the resiliency of our cooperative optimization based on electricity price prediction, cost reduction of distributed energy resources such that batteries and DG units for the main objective to reduce the total economic operating costs while satisfying supply-demand balance.

## VII. CONCLUSION

In this paper, a novel real-time optimization based on a data-predictive control framework is proposed for the new generation of the energy management system (RDPC-EMS). In the first stage, a learning algorithm based on the OR-ELM model is employed for an accurate electricity retail price forecasting by reducing outlier effects on the training data modeling and the stochastic model identification problem for the electricity markets market. The historical pricing dataset have been collected from the ISO New England market based on the marginal price concept, evaluation performance demonstrates the robustness of OR-ELM compared to the SVR and ANN models. In the second part of our work, we apply the cooperative distributed MPC optimization to

solve the MMG community economic energy dispatch and management. First, The distribution system operator DSO is considered as the first-level which solve the energy management problem based on DMPC optimization, considering the predicted electricity price by OR-ELM learning algorithm, and broadcasting the optimal energy scheduling solution for one day ahead to the LC-MG. In the second level, the local controller execute the energy scheduled by setting up the controllable distributed energy resources DER, such as energy storage systems and DG units, to maintain the MG supply-demand balance. The energy surplus energy is exchanged among the MMG network, which decrease the operation cost by a reduced amount of electricity purchasing from the Main Grid. Furthermore, our method's advantage is resiliency for active load distribution in both cooperative and non-cooperative scenarios. However, the operating cost is higher for the non-cooperative scenarios with an increase of 15% for MG 1 and 16% for MG 2.

Future work will follow this paper to further investigate some important points which have not been addressed in our study. For instance, including the operating costs for renewable energy, such as the operation and maintenance of the PV solar panels, and study their impact on the economic dispatch for microgrids systems with high integration of renewable resources. Further, investigate the OR-ELM learning algorithm model for the load demand and renewable energy resources uncertainties for the economic energy dispatching.

## REFERENCES

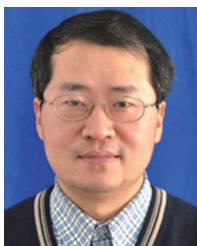
- [1] P. A. Østergaard, R. M. Johannsen, and N. Duic, "Sustainable development using renewable energy systems," *Int. J. Sustain. Energy Planning Manage.*, vol. 29, pp. 1–6, Sep. 2020.
- [2] B. Chen, J. Wang, X. Lu, C. Chen, and S. Zhao, "Networked microgrids for grid resilience, robustness, and efficiency: A review," *IEEE Trans. Smart Grid*, vol. 12, no. 1, pp. 18–32, Jan. 2021.
- [3] S. Wang, X. Zhang, L. Wu, and S. Sun, "New metrics for assessing the performance of multi-microgrid systems in stand-alone mode," *Int. J. Electr. Power Energy Syst.*, vol. 98, pp. 382–388, Jun. 2018.
- [4] S. Charani Shandiz, G. Foliente, B. Rismanchi, A. Wachtel, and R. F. Jeffers, "Resilience framework and metrics for energy master planning of communities," *Energy*, vol. 203, Jul. 2020, Art. no. 117856.
- [5] A. A. Anderson and S. Suryanarayanan, "Review of energy management and planning of islanded microgrids," *CSEE J. Power Energy Syst.*, vol. 6, no. 2, pp. 329–343, 2019.

- [6] H. R. Gholinejad, A. Loni, J. Adabi, and M. Marzband, "A hierarchical energy management system for multiple home energy hubs in neighborhood grids," *J. Building Eng.*, vol. 28, Mar. 2020, Art. no. 101028.
- [7] S. E. Ahmadi, N. Rezaei, and H. Khayyam, "Energy management system of networked microgrids through optimal reliability-oriented day-ahead self-healing scheduling," *Sustain. Energy, Grids Netw.*, vol. 23, Sep. 2020, Art. no. 100387.
- [8] F. S. Gazijahani, S. N. Ravadanegh, and J. Salehi, "Stochastic multi-objective model for optimal energy exchange optimization of networked microgrids with presence of renewable generation under risk-based strategies," *ISA Trans.*, vol. 73, pp. 100–111, Feb. 2018.
- [9] H. Fu and X.-P. Zhang, "Market equilibrium in active distribution system with  $\mu$  VPPs: A coevolutionary approach," *IEEE Access*, vol. 5, pp. 8194–8204, 2017.
- [10] M. Ahmed, L. Meegahapola, A. Vahidnia, and M. Datta, "Stability and control aspects of microgrid architectures—A comprehensive review," *IEEE Access*, vol. 8, pp. 144730–144766, 2020.
- [11] M. Islam, F. Yang, C. Ekanayek, and M. Amin, "Grid power fluctuation reduction by fuzzy control based energy management system in residential microgrids," *Int. Trans. Electr. Energy Syst.*, vol. 29, no. 3, Mar. 2019, Art. no. e2758.
- [12] X. Liu, B. Gao, Z. Zhu, and Y. Tang, "Non-cooperative and cooperative optimisation of battery energy storage system for energy management in multi-microgrid," *IET Gener., Transmiss. Distrib.*, vol. 12, no. 10, pp. 2369–2377, May 2018.
- [13] L. Yin, T. Yu, B. Yang, and X. Zhang, "Adaptive deep dynamic programming for integrated frequency control of multi-area multi-microgrid systems," *Neurocomputing*, vol. 344, pp. 49–60, Jun. 2019.
- [14] A. Papavasiliou, Y. Mou, L. Cambier, and D. Scieur, "Application of stochastic dual dynamic programming to the real-time dispatch of storage under renewable supply uncertainty," *IEEE Trans. Sustain. Energy*, vol. 9, no. 2, pp. 547–558, Apr. 2018.
- [15] D. Mariano-Hernández, L. Hernández-Callejo, A. Zorita-Lamadrid, O. Duque-Pérez, and F. Santos García, "A review of strategies for building energy management system: Model predictive control, demand side management, optimization, and fault detect & diagnosis," *J. Building Eng.*, vol. 33, Jan. 2021, Art. no. 101692.
- [16] A. Parisio, C. Wiezorek, T. Kytäjä, J. Elo, K. Strunz, and K. H. Johansson, "Cooperative MPC-based energy management for networked microgrids," *IEEE Trans. Smart Grid*, vol. 8, no. 6, pp. 3066–3074, Nov. 2017.
- [17] C. Wu, S. Gao, Y. Liu, T. E. Song, and H. Han, "A model predictive control approach in microgrid considering multi-uncertainty of electric vehicles," *Renew. Energy*, vol. 163, pp. 1385–1396, Jan. 2021.
- [18] B. E. Sedhom, M. M. El-Saadawi, A. Y. Hatata, and A. S. Alsayyari, "Hierarchical control technique-based harmony search optimization algorithm versus model predictive control for autonomous smart microgrids," *Int. J. Electr. Power Energy Syst.*, vol. 115, Feb. 2020, Art. no. 105511.
- [19] N. Bazmohammadi, A. Tahsiri, A. Anvari-Moghaddam, and J. M. Guerrero, "A hierarchical energy management strategy for interconnected microgrids considering uncertainty," *Int. J. Electr. Power Energy Syst.*, vol. 109, pp. 597–608, Jul. 2019.
- [20] N. Bazmohammadi, A. Anvari-Moghaddam, A. Tahsiri, A. Madary, J. C. Vasquez, and J. M. Guerrero, "Stochastic predictive energy management of multi-microgrid systems," *Appl. Sci.*, vol. 10, no. 14, p. 4833, Jul. 2020.
- [21] N. Bazmohammadi, A. Tahsiri, A. Anvari-Moghaddam, and J. M. Guerrero, "Stochastic predictive control of multi-microgrid systems," *IEEE Trans. Ind. Appl.*, vol. 55, no. 5, pp. 5311–5319, Sep. 2019.
- [22] M. Legry, F. Colas, C. Saudemont, J. Y. Dieulot, and O. Ducarme, "A two-layer model predictive control based secondary control with economic performance tracking for islanded microgrids," in *Proc. IECON 44th Annu. Conf. IEEE Ind. Electron. Soc.*, Oct. 2018, pp. 77–82.
- [23] M. Tavakoli, F. Shokridehaki, M. Marzband, R. Godina, and E. Pouresmaeil, "A two stage hierarchical control approach for the optimal energy management in commercial building microgrids based on local wind power and PEVs," *Sustain. Cities Soc.*, vol. 41, pp. 332–340, Aug. 2018.
- [24] M. Razzanelli, E. Crisostomi, L. Pallottino, and G. Pannocchia, "Distributed model predictive control for energy management in a network of microgrids using the dual decomposition method," *Optim. Control Appl. Methods*, vol. 41, no. 1, pp. 25–41, Jan. 2020.
- [25] W. Ananduta, J. M. Maestre, C. Ocampo-Martinez, and H. Ishii, "Resilient distributed model predictive control for energy management of interconnected microgrids," *Optim. Control Appl. Methods*, vol. 41, no. 1, pp. 146–169, Jan. 2020.
- [26] Y. Du, J. Wu, S. Li, C. Long, and I. C. Paschalidis, "Distributed MPC for coordinated energy efficiency utilization in microgrid systems," *IEEE Trans. Smart Grid*, vol. 10, no. 2, pp. 1781–1790, Mar. 2019.
- [27] Y. Sun, F. Haghighat, and B. C. M. Fung, "A review of the-state-of-the-art in data-driven approaches for building energy prediction," *Energy Buildings*, vol. 221, Aug. 2020, Art. no. 110022.
- [28] S. Atef and A. B. Eltawil, "A comparative study using deep learning and support vector regression for electricity price forecasting in smart grids," in *Proc. IEEE 6th Int. Conf. Ind. Eng. Appl. (ICIEA)*, Apr. 2019, pp. 603–607.
- [29] C. Li, S. Li, and Y. Liu, "A least squares support vector machine model optimized by moth-flame optimization algorithm for annual power load forecasting," *Int. J. Speech Technol.*, vol. 45, no. 4, pp. 1166–1178, Dec. 2016.
- [30] H. Cai, S. Shen, Q. Lin, X. Li, and H. Xiao, "Predicting the energy consumption of residential buildings for regional electricity supply-side and demand-side management," *IEEE Access*, vol. 7, pp. 30386–30397, 2019.
- [31] S. Zhou, L. Zhou, M. Mao, H.-M. Tai, and Y. Wan, "An optimized heterogeneous structure LSTM network for electricity price forecasting," *IEEE Access*, vol. 7, pp. 108161–108173, 2019.
- [32] S. Esmaili, A. Anvari-Moghaddam, and S. Jadid, "Retail market equilibrium and interactions among reconfigurable networked microgrids," *Sustain. Cities Soc.*, vol. 49, Aug. 2019, Art. no. 101628.
- [33] S. Trueck, R. Weron, and R. Wolff, "Outlier treatment and robust approaches for modeling electricity spot prices," Univ. Library Munich, Munich, Germany, Tech. Rep., 2007.
- [34] J. Wang, W. Yang, P. Du, and T. Niu, "Outlier-robust hybrid electricity price forecasting model for electricity market management," *J. Cleaner Prod.*, vol. 249, Mar. 2020, Art. no. 119318.
- [35] M. Hossain, S. Mekhilef, M. Danesh, L. Olatomiwa, and S. Shamshirband, "Application of extreme learning machine for short term output power forecasting of three grid-connected PV systems," *J. Cleaner Prod.*, vol. 167, pp. 395–405, Nov. 2017.
- [36] D. Koolen, N. Sadat-Razavi, and W. Ketter, "Machine learning for identifying demand patterns of home energy management systems with dynamic electricity pricing," *Appl. Sci.*, vol. 7, no. 11, p. 1160, Nov. 2017.
- [37] F. Smarra, A. Jain, T. de Rubeis, D. Ambrosini, A. D'Innocenzo, and R. Mangharam, "Data-driven model predictive control using random forests for building energy optimization and climate control," *Appl. Energy*, vol. 226, pp. 1252–1272, Sep. 2018.
- [38] I. Brahmia, P. Zhao, and J. Wang, "Efficient energy management of multi-microgrids systems based on distributed cooperative control in autonomous mode," in *Proc. 9th Int. Conf. Power Energy Syst. (ICPES)*, Dec. 2019, pp. 1–6.
- [39] I. Brahmia, J. Wang, S. Yuanhao, and L. Yang, "Smart energy dispatch for networked microgrids systems based on distributed control within a hierarchy optimization," in *Proc. IFAC World Congress Int. Fed. Automatic Control*, 2020, pp. 13182–13187.
- [40] B. Zhao, Y. Li, and R. Wang, "Solar PV powered heating and cooling," early access, 2020.
- [41] *ISO New England Pricing Reports Real-Time Hourly LMPs*. Accessed: Jul. 1, 2020. [Online]. Available: <https://www.iso-ne.com>
- [42] A. Parisio, E. Rikos, G. Tzamalís, and L. Glielmo, "Use of model predictive control for experimental microgrid optimization," *Appl. Energy*, vol. 115, pp. 37–46, Feb. 2014.
- [43] M. Zhai, Y. Liu, T. Zhang, and Y. Zhang, "Robust model predictive control for energy management of isolated microgrids," in *Proc. IEEE Int. Conf. Ind. Eng. Eng. Manage. (IEEM)*, Dec. 2017, pp. 2049–2053.
- [44] J. Sachs and O. Sawodny, "A two-stage model predictive control strategy for economic Diesel-PV-Battery island microgrid operation in rural areas," *IEEE Trans. Sustain. Energy*, vol. 7, no. 3, pp. 903–913, Jul. 2016.
- [45] A. Parisio, E. Rikos, and L. Glielmo, "A model predictive control approach to microgrid operation optimization," *IEEE Trans. Control Syst. Technol.*, vol. 22, no. 5, pp. 1813–1827, Sep. 2014.
- [46] S. Shamshirband, K. Mohammadi, C. W. Tong, D. Petković, E. Porcu, A. Mostafaeipour, S. Ch, and A. Sedaghat, "RETRACTED ARTICLE: Application of extreme learning machine for estimation of wind speed distribution," *Climate Dyn.*, vol. 46, nos. 5–6, pp. 1893–1907, Mar. 2016.

- [47] K. Zhang and M. Luo, "Outlier-robust extreme learning machine for regression problems," *Neurocomputing*, vol. 151, pp. 1519–1527, Mar. 2015.
- [48] J. M. Martínez-Martínez, P. Escandell-Montero, E. Soria-Olivas, J. D. Martín-Guerrero, R. Magdalena-Benedito, and J. Gómez-Sanchis, "Regularized extreme learning machine for regression problems," *Neurocomputing*, vol. 74, no. 17, pp. 3716–3721, Oct. 2011.
- [49] S. Nematshahi and H. R. Mashhadi, "Application of distribution locational marginal price in optimal simultaneous distributed generation placement and sizing in electricity distribution networks," *Int. Trans. Electr. Energy Syst.*, vol. 29, no. 5, May 2019, Art. no. e2837.
- [50] A. Almuhtady, A. Alshwawra, M. Alfaouri, W. Al-Kouz, and I. Al-Hinti, "Investigation of the trends of electricity demands in Jordan and its susceptibility to the ambient air temperature towards sustainable electricity generation," *Energy, Sustainability Soc.*, vol. 9, no. 1, pp. 1–18, Dec. 2019.
- [51] A. N. Venkat, "Distributed model predictive control: Theory and applications," Ph.D. dissertation, Univ. Wisconsin-Madison, Madison, WI, USA, 2006.
- [52] A. N. Venkat, I. A. Hiskens, J. B. Rawlings, and S. J. Wright, "Distributed MPC strategies with application to power system automatic generation control," *IEEE Trans. Control Syst. Technol.*, vol. 16, no. 6, pp. 1192–1206, Nov. 2008.
- [53] *Residential Hourly Load Profiles for all Tmy3 Locations in the United States*, E. Commercial, US Department of Energy Office of Energy Efficiency & Renewable Energy (EERE), Washington, DC, USA, Jul. 2013, vol. 2.



**IBRAHIM BRAHMIA** received the B.S. and M.S. degrees from the Institute for Aeronautics and Aerospace Studies, Algeria, in 2011 and 2013, respectively. He is currently pursuing the Ph.D. degree with the Department of Automation, Shanghai Jiao Tong University, Shanghai, China. His current research interests include real time dynamic simulation and robust control, intelligent information processing, data analysis, and modeling optimization for cyber-physical systems.



**JINGCHENG WANG** received the B.S. and M.S. degrees from Northwestern Polytechnic University, Xi'an, China, in 1992 and 1995, respectively, and the Ph.D. degree from Zhejiang University, Hangzhou, China, in 1998.

He is a Former Research Fellow with the Alexander von Humboldt Foundation, Rostock University, Rostock, Germany. He is currently a Professor with Shanghai Jiao Tong University, Shanghai, China. His current research inter-

ests include robust control, intelligent control, and real-time control and simulation.

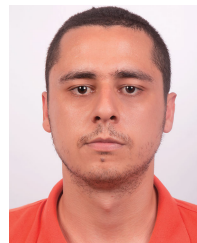


**HAOTIAN XU** received the B.S. degree from the School of Mathematics, Shandong University, China, in 2016. He is currently pursuing the Ph.D. degree with the Department of Automation, Shanghai Jiao Tong University, Shanghai, China.

His current research interests include nonlinear control, distributed control and observer, and partial observer canonical form.



**HONGYUAN WANG** received the B.S. degree from the College of Electrical and Information Engineering, Hunan University, Changsha, China, in 2015. He is currently pursuing the Ph.D. degree with the Department of Automation, Shanghai Jiao Tong University, Shanghai, China. His current research interest includes stochastic/robust model predictive control.



**LUCA DE OLIVEIRA TURCI** received the Control and Automation Engineering degree from the Universidade Federal de Ouro Preto, Ouro Preto, Brazil, in 2016, and the M.Sc. degree in control science and engineering from Shanghai Jiao Tong University, China, in 2020. He was a member of the Control Science and Automation Department, whereas developed this project.

...